

# Observation of a Structure in $pp \rightarrow pp\gamma\gamma$ near the $\pi\pi$ Threshold and its Possible Interpretation by $\gamma\gamma$ Radiation from Chiral Loops in the Mesonic $\sigma$ Channel

M. Bashkanov<sup>1</sup>, D. Bogoslawsky<sup>2</sup>, H. Calén<sup>3</sup>, F. Cappellaro<sup>4</sup>, H. Clement<sup>1</sup>, L. Demiroers<sup>5</sup>, E. Doroshkevich<sup>1</sup>, C. Ekström<sup>3</sup>, K. Fransson<sup>3</sup>, J. Greiff<sup>5</sup>, L. Gustafsson<sup>4</sup>, B. Höistad<sup>4</sup>, G. Ivanov<sup>2</sup>, M. Jacewicz<sup>4</sup>, E. Jiganov<sup>2</sup>, T. Johansson<sup>4</sup>, M.M. Kaskulov<sup>1</sup>, S. Keleta<sup>4</sup>, I. Koch<sup>4</sup>, S. Kullander<sup>4</sup>, A. Kupść<sup>3</sup>, A. Kuznetsov<sup>2</sup>, P. Marciniewski<sup>3</sup>, R. Meier<sup>1</sup>, B. Morosov<sup>2</sup>, W. Oelert<sup>8</sup>, C. Pauly<sup>5</sup>, Y. Petukhov<sup>2</sup>, A. Povtorejko<sup>2</sup>, R.J.M.Y. Ruber<sup>3</sup>, W. Scobel<sup>5</sup>, B. Schwartz<sup>10</sup>, T. Skorodko<sup>1</sup>, V. Sopov<sup>12</sup>, J. Stepaniak<sup>7</sup>, V. Tchernyshev<sup>12</sup>, P. Thörngren Engblom<sup>4</sup>, V. Tikhomirov<sup>2</sup>, A. Turowiecki<sup>11</sup>, G.J. Wagner<sup>1</sup>, U. Wiedner<sup>4</sup>, M. Wolke<sup>4</sup>, A. Yamamoto<sup>6</sup>, J. Zabierowski<sup>7</sup>, J. Zlomanczuk<sup>4</sup>

<sup>1</sup>*Physikalisches Institut der Universität Tübingen,*

*D-72076 Tübingen, Germany*

<sup>2</sup>*Joint Institute for Nuclear Research, Dubna, Russia*

<sup>3</sup>*The Svedberg Laboratory, Uppsala, Sweden*

<sup>4</sup>*Uppsala University, Uppsala, Sweden*

<sup>5</sup>*Hamburg University, Hamburg, Germany*

<sup>6</sup>*High Energy Accelerator Research Organization, Tsukuba, Japan*

<sup>7</sup>*Soltan Institute of Nuclear Studies,*

*Warsaw and Lodz, Poland*

<sup>8</sup>*Forschungszentrum Jülich, Germany*

<sup>9</sup>*Moscow Engineering Physics Institute, Moscow, Russia*

<sup>10</sup>*Budker Institute of Nuclear Physics, Novosibirsk, Russia*

<sup>11</sup>*Institute of Experimental Physics, Warsaw, Poland*

<sup>12</sup>*Institute of Theoretical and Experimental Physics, Moscow, Russia*

(CELSIUS-WASA Collaboration)

(Dated: November 20, 2018)

The  $pp \rightarrow pp\gamma\gamma$  reaction has been measured at CELSIUS using the WASA 4 $\pi$ -detector with hydrogen pellet target. At  $T_p = 1.20$  and 1.36 GeV, where most of the statistics has been accumulated, the  $\gamma\gamma$  invariant mass spectrum exhibits a narrow structure around the  $\pi\pi$  threshold, which possibly may be associated with two-photon radiation of  $\pi^+\pi^-$  loops in the mesonic  $\sigma$  channel.

PACS numbers: 13.75.Cs, 14.20.Gk, 14.40.Aq, 14.40.Cs

The question whether there exists a low-lying scalar-isoscalar resonance in the  $\pi\pi$  system, the so-called  $\sigma$ -meson, has a long history. Starting from the  $\sigma$  particle problem in nuclear physics, where such an exchange particle (possibly in form of a correlated  $\pi\pi$  exchange) is needed to accommodate for the scalar-isoscalar attraction in the  $NN$  interaction, the quest for the  $\sigma$ -meson has found renewed interest in QCD as the chiral partner of the pion — and in this context possibly even as the Higgs particle of the strong interaction [1]. Also the scalar-isoscalar meson sector is under much debate presently, since there are more states known meanwhile (including also possible glueball candidates) than can be fitted into a single multiplet. Hence it has been suggested [2], that there are actually two nonets, a higher-lying one of predominant  $q\bar{q}$  nature and a lower-lying one, encompassing the  $\sigma$  meson, of dominant  $q\bar{q}q\bar{q}$  structure. This picture of the  $\sigma$  would be also close to the result of chiral perturbation theory, where the  $\sigma$  emerges dynamically in  $\pi\pi$  rescattering [3, 4, 5].

Experimentally the  $\sigma$  is very hard to sense because of its expected huge width due to its fall-apart decay into  $\pi\pi$ . Besides of  $\pi\pi$  phase shifts recent experiments on  $J/\psi \rightarrow \omega\pi^+\pi^-$  [6],  $D^+ \rightarrow \pi^-\pi^+\pi^+$  [7] and  $\tau \rightarrow \nu_\tau\pi^-\pi^0\pi^0$  [8] have added evidence for the existence

of  $\sigma$  with a mass in the range 320-480 MeV and a width of roughly the same size. To learn more specifically about the nature of the  $\sigma$  meson, its decay into two gammas would be of great help, since this would directly give evidence for tight particle-antiparticle correlations influencing heavily the annihilation radiation [9, 10, 11, 12]. In fact, measurements [10, 11] of double pion production in  $e^+e^- \rightarrow \gamma^*\gamma^* \rightarrow \pi\pi$  have been used to get access to the  $\sigma \rightarrow \gamma\gamma$  decay [9, 12]. At energies near the  $\pi\pi$  threshold these reactions are governed by pion production through the Born terms. In a theoretical analysis of these data a possible contribution of  $\gamma^*\gamma^* \rightarrow \sigma \rightarrow \pi\pi$  has been investigated and a value of  $\Gamma_{\sigma \rightarrow \gamma\gamma}/\Gamma_{\sigma \rightarrow \pi\pi} \approx 10^{-6}$  has been extracted [9, 12] at the pole of the  $\sigma$ .

We have carried out measurements of the reaction  $pp \rightarrow pp\gamma\gamma$  at the CELSIUS ring in the energy range of  $T_p = 775 - 1360$  MeV using the WASA detector together with the pellet hydrogen target system [13]. The detector has nearly full angular coverage for the detection of charged and uncharged particles. The forward detector consists of a straw tracker unit followed by plastic scintillator quirl and range hodoscopes, whereas the central detector comprises in its inner part a thin-walled superconducting magnet containing a minidrift chamber for tracking, and in its outer part a plastic scintillator barrel

surrounded by an electromagnetic calorimeter consisting of 1012 CsI(Na) crystals. In these runs triggers had been set to allow also for simultaneous measurements of single pion, double pion and — in case of the highest energy — also  $\eta$ -production. In case of  $pp \rightarrow pp\gamma\gamma$  the two protons have been detected in the forward detector, whereas the gammas have been detected in the central detector. This way the full four-momenta have been measured for all particles, allowing thus kinematic fits for each event with 4 overconstraints. Also in order to be safe from events, where particles have escaped detection, we require the total energy of the detected particles (before kinematic fit) to be equal to that in the entrance channel within 100 MeV, i.e. within a difference smaller than the pion mass. To suppress background further we in addition accept only photons with  $E_\gamma > 50$  MeV for the final event samples.

The by far highest statistics has been accumulated at  $T_p = 1.36$  GeV, hence we concentrate in the following on this energy. Fig. 1a shows a scatter plot of the  $\gamma\gamma$  invariant mass  $M_{\gamma\gamma}$  versus the pp missing mass  $MM_{pp}$  for the selected events. The photon energy resolution is best for small energies, hence the resolution in  $M_{\gamma\gamma}$  is best at low energies. The situation is reversed in  $MM_{pp}$ , since the protons undergo hadronic interactions in the detector increasingly with increasing energy. Careful inspection of this plot exhibits already evidence for some enhanced rate between the spots for  $\pi^0$  and  $\eta$ . In order to clean the sample from events, where the protons have undergone very large hadronic interactions, we employ the condition  $(M_{\gamma\gamma} - MM_{pp})/MM_{pp} < 0.4$ . The emerging projection of the scatterplot onto the  $M_{\gamma\gamma}$  axis is shown in Fig. 1b. A peak-like structure around the  $\pi\pi$  threshold appears now clearly visible. Finally a kinematic fit ( without imposing conditions for the final meson mass ) is applied to the sample, resulting (Fig. 1c) primarily in a reduction of the width of the peaks, in particular of the  $\eta$  peak. The resulting full width at half maximum is  $\approx 22$  MeV for  $\pi^0$  and  $\eta$  peaks. The width of the structure at the  $\pi\pi$  threshold also is consistent with this value.

An important check whether the peak-like structure could be of instrumental origin may be provided by measurements under different kinematical conditions. To this end we have analyzed in the same way data accumulated at lower energies and found evidence for this spike also at  $T_p = 1.2$  GeV (Fig. 1d) despite the lower statistics there.

This spike turns out to be very stable against cuts. E.g., increase of the threshold  $E_\gamma = 50$  MeV to  $E_\gamma = 100$  MeV has no significant effect on this spike. MC simulations for  $\pi^0$  and  $\eta$  production providing a good reproduction of the respective peaks in  $M_{\gamma\gamma}$  give no evidence for a scatter of counts (stemming from these reactions) into the region between the two peaks. Also from simulation of  $\pi^+\pi^-$  production we do not get any contributions in the  $M_{\gamma\gamma}$  spectrum. Solely the MC simulation of  $\pi^0\pi^0$  production does give some scatter of counts into this region stemming from  $pp\pi^0\pi^0 \rightarrow pp\gamma\gamma\gamma\gamma$  events, where two

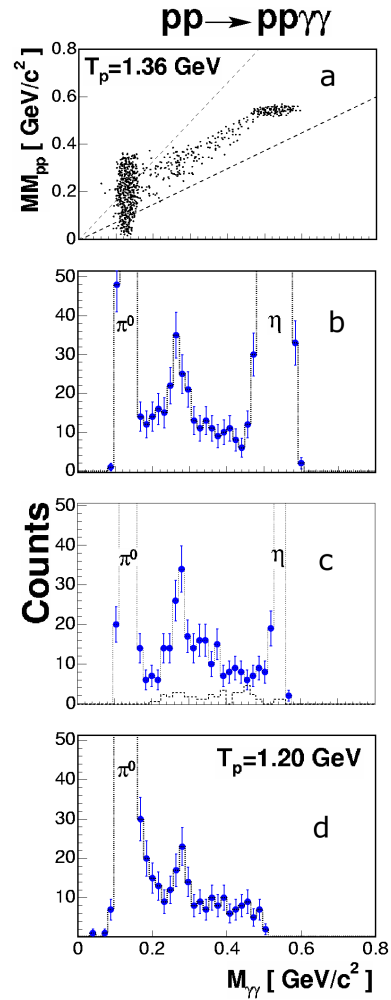


FIG. 1: (a): Scatterplot of  $M_{\gamma\gamma}$  versus the  $MM_{pp}$  for all selected events at  $T_p = 1.36$  GeV. The dashed line shows the cut  $(M_{\gamma\gamma} - MM_{pp})/MM_{pp} < 0.4$  to exclude events, where protons have undergone large hadronic interactions in the detector. (b) - (c):  $M_{\gamma\gamma}$  spectrum (projection of the scatterplot above) before (b) and after (c) kinematic fit. The dotted histogram in (c) shows background expected from misidentified  $\pi^0\pi^0$  events. (d): The same as (c), but for  $T_p = 1.2$  GeV.

low-energy  $\gamma$ s have escaped detection in WASA. In fact, taking into account the absolute cross section of  $\approx 200\mu\text{b}$  for the  $\pi^0\pi^0$  production at 1.36 GeV [19, 20] about 15% of the observed counts between  $\pi^0$  and  $\eta$  peaks are compatible with misidentified  $pp\pi^0\pi^0$  events ( see dotted histogram in fig. 1c ). The most dangerous situation for producing an artefact peak at  $2m_\pi$  is, if two  $\pi^0$ s decay in such a similar manner that the clusters produced by their  $\gamma$ s just merge pairwise into each other. However, such a constellation, which is included in the MC simulations shown in fig. 1c, dotted line, is too rare to produce an enhancement at  $2m_\pi$ . We also have investigated this special scenario with real  $\pi^0\pi^0$  data by deliberately merging clusters. Again this operation did not result in a reproduction of the observed structure.

Since none of these simulated processes is able to account for the structure observed near the  $\pi\pi$  threshold and also detailed and comprehensive tests of detector performance and event structures have not given any hint for an artifact, we are led to consider seriously the possibility that the observed structure is real and might be due to the process  $pp \rightarrow pp\sigma \rightarrow pp\gamma\gamma$ , in particular also since  $pp \rightarrow pp\pi^+\pi^-$  and  $pp \rightarrow pp\pi^0\pi^0$  reactions are dominated by  $\sigma$  production [14, 15].

The statistical significance of the spike observed at the  $\pi\pi$  threshold may be estimated directly by inspection of Fig. 1. There we see that the spike contains roughly  $N_S \approx 60$  counts above a background of  $N_B \approx 60$  counts at  $T_p = 1.36$  GeV. The significance in standard deviations depends on the assumption about the background behaviour. Neglect of the statistical fluctuations of the background gives  $S = N_S/\sqrt{N_B} \approx 7.7$ . A more reliable estimate is  $S = N_S/\sqrt{N_S + N_B} \approx 5.5$ , assuming a fluctuating background, which is smooth and well-fixed in shape. Finally, assuming the full uncertainty of a statistically independent background results in  $S = N_S/\sqrt{N_S + 2 * N_B} \approx 4.5$ . Somewhat lower values arise, if we use the data at  $T_p = 1.2$  GeV, where  $N_S \approx N_B \approx 30$ .

We note that recently the  $\sigma \rightarrow \gamma\gamma$  decay has also been searched for [16] in  $^{12}\text{C}(\pi^-, \pi^0\pi^0)$ . The  $M_{\gamma\gamma}$  spectrum shown there exhibits some indication of a gentle enhancement near  $2m_\pi$ . Though this reaction cannot directly be compared to our case, it is worth noting that the quoted relative upper limit is of similar order of magnitude as our observation.

We next inspect the efficiency and acceptance corrected angular distributions. For these we reconstruct the  $\pi^0$ ,  $\eta$  and  $\sigma$  momenta from the respective  $\gamma$  pairs. The angular distributions  $\sigma(\Theta_{CM})$  of these reconstructed momenta in the overall center of mass system are plotted in Fig. 2. For  $\pi^0$  we obtain an angular distribution close to  $(1 + 3\cos^2\Theta_{CM})$  consistent with  $\Delta$  and Roper resonance excitations in  $pp \rightarrow pp\pi^0$ . For  $\eta$  we see an s-wave behavior consistent with the excitation of the  $S_{11}(1535)$  resonance in  $pp \rightarrow pp\eta$  and also in agreement with previous measurements [17, 18]. And for the spike region we obtain a flat angular distribution, too, again consistent with s-wave production.

In order to get absolute cross sections we have for convenience normalized our data for the  $\eta$  peak to the well-known cross section of  $4.9\mu\text{b}$  for  $pp \rightarrow pp\eta$  at  $T_p = 1.36$  GeV [17], which by use of the known  $\eta \rightarrow \gamma\gamma$  branching ratio of 39% [9] results in a cross section of  $1.9\mu\text{b}$  for  $pp \rightarrow pp\eta \rightarrow pp\gamma\gamma$ . This normalization then leads to a cross section value of  $4\text{ mb}$  for  $pp \rightarrow pp\pi^0$  which is in reasonable agreement with previous measurements [19]. For the structure around the  $\pi\pi$  threshold the quotation of an absolute cross section depends crucially on the assumption of background beneath this structure. If we just take the narrow spike above the smooth continuum, then we arrive at roughly  $1 - 2\mu\text{b}$  for its cross section. The acceptance and efficiency corrected as well as nor-

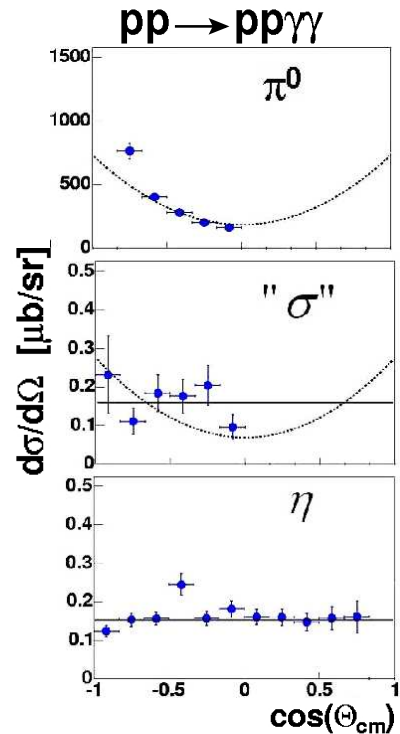


FIG. 2: Angular distributions of the  $\gamma\gamma$  pair momentum in the overall cms for  $\gamma$ s belonging to  $\pi^0$  peak,  $\eta$  peak and to the spike region, respectively. The solid lines show fits with  $\sigma(\Theta_{CM}) \sim 1 + 3\cos^2\Theta_{CM}$  for  $\pi^0$  and  $\sigma(\Theta_{CM}) = \text{constant}$  otherwise.

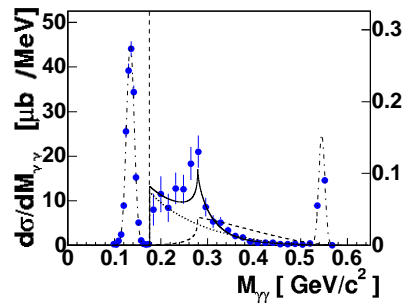


FIG. 3: Differential cross section in dependence of  $M_{\gamma\gamma}$ . Note the change of scale at  $M_{\gamma\gamma} = 0.18\text{ GeV}/c^2$  by more than a factor of 100! The dotted curve shows MC simulations for double bremsstrahlung adjusted in height to the data. The dashed line gives calculations of the diagrams in Fig. 4, whereas the solid line represents their coherent sum.

malized  $M_{\gamma\gamma}$  spectrum is shown in Fig. 3.

A process which principally contributes to the energy region of interest is double bremsstrahlung. Single bremsstrahlung has been calculated [21] at  $T_p = 1.35$  GeV to give a total cross section of about  $100\mu\text{b}$  for  $E_\gamma > 100$  MeV. For double bremsstrahlung we are not aware of any such detailed calculation. However, we may obtain a first crude estimate for its cross section by just multiplying the single bremsstrahlung result with

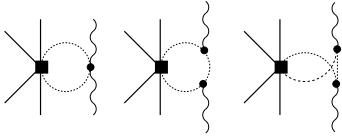


FIG. 4: Graphs for the dynamical formation of s-wave virtual  $\pi^+\pi^-$  loops generated in the  $pp$  collision process and its subsequent annihilation into two photons.

the fine structure constant  $\alpha$ . This estimate presumably will only be a lower limit, since there are much more different diagrams contributing to double than to single bremsstrahlung. Anyway from these considerations we may expect the double bremsstrahlung cross section to be of the same order of magnitude as given by the observed continuum of counts between  $\pi^0$  and  $\eta$  peaks. Though double bremsstrahlung certainly cannot explain the narrow spike, it appears to be a good candidate for explaining the continuum beneath the spike. The dotted lines in Fig. 3 shows a MC simulation for this process adjusted in height to the data and assuming  $d\sigma/dM_{\gamma\gamma} \sim M_{\gamma\gamma}^{-1}$  [22].

Qualitatively a cusp-like energy dependence of the process  $pp \rightarrow pp\sigma \rightarrow pp\gamma\gamma$  can be obtained by a Breit-Wigner ansatz  $d\sigma/dM_{\gamma\gamma} \sim (\varepsilon^2 + \Gamma^2/4)^{-1}$  with  $\varepsilon = M_{\gamma\gamma} - m_\sigma$  and the (energy dependent) total width  $\Gamma = \Gamma_{\gamma\gamma} + \Gamma_{\pi\pi}$ . Below the  $\pi\pi$  threshold we have  $\Gamma = \Gamma_{\gamma\gamma} \approx 10^{-6}\Gamma_{\pi\pi}$  and above  $\Gamma \approx \Gamma_{\pi\pi}$ . For  $m_\sigma \approx \Gamma_{\pi\pi} \approx 350\text{MeV}$  we this way arrive at a qualitative description of the observed structure.

To discuss the possible origin of the spike on a more fundamental level, we consider the graphs in Fig. 4, where correlations in the  $\sigma$  channel are formed dynamically by pion loops generated in the  $pp$  collision process and coupled to the  $\gamma\gamma$  channel. The blob represents the generation of virtual pion pairs and may be adjusted in scale to the total hadronic  $pp$  cross section at  $T_p = 1.36$

GeV. Evaluation of the loop diagrams with a branch cut at the  $\pi^+\pi^-$  threshold [23], leads to a cusp-like structure (dashed lines in Fig. 3) with a strength basically of order  $\alpha^2$  smaller than the total cross section. Though we arrive at the proper order of magnitude for the effect under discussion, the predicted shape is still quite different. However, this amplitude is to interfere with the one for double bremsstrahlung. With a proper choice for the relative phase between both processes we obtain a curve, which fits the data remarkably well (solid lines in Fig. 3). Note that this cusp effect due to  $\gamma\gamma$  radiation induced by recombination of chiral loops is very general and should appear principally also in channels other than the  $\sigma$  channel discussed here.

Summarizing we observe a narrow spike around the  $\pi\pi$  threshold in the  $M_{\gamma\gamma}$  spectrum of the  $pp \rightarrow pp\gamma\gamma$  reaction. Its angular distribution is consistent with s-wave production. In a first attempt for its interpretation we consider  $\sigma$  channel pion loops, which are generated by the  $pp$  collision process and which decay into the  $\gamma\gamma$  channel. Chiral loop calculations of this process reveal indeed a cusp-like behaviour, which by interference with the underlying double bremsstrahlung background can give a reasonable account of the data. If true then this observation would be a manifestation of a correlated  $\pi\pi$  system in the  $\sigma$  channel. The correlated  $\pi\pi$  exchange between nucleons [24, 25] would not need to be lifted above the  $\pi\pi$  threshold to get on mass shell, it would be so already below this threshold with respect to the  $\gamma\gamma$  decay channel. Similar loop effects are expected to show up also in other channels.

We are grateful to the TSL/ISV personnel for the continued help during the course of these measurements. This work has been supported by BMBF (06TU201), DFG (Europ. Graduiertenkolleg 683) and Baden-Wuerttemberg Landesforschungsschwerpunkt.

- 
- [1] M.R. Pennington, hep-ph/9905241, Proc. Workshop on Hadron Spectroscopy, Frascati 1999, 95
  - [2] F.E. Close and N.A. Törnquist, J. Phys. **G28**, R249 (2002)
  - [3] G. Colangelo, J. Gasser and H. Leutwyler, Nucl. Phys. **B603**, 125 (2001)
  - [4] J.A. Oller, E. Oset and J.R. Pelàez, Phys. Rev. Lett. **80**, 3452 (1998), Phys. Rev. **D59**, 074001 (1999)
  - [5] J.R. Pelàez, Phys. Rev. Lett. **92**, 102001 (2004)
  - [6] Ning Wu, hep-ex/0104050
  - [7] E.M. Aitala et al., Phys. Rev. Lett. **86**, 770 (2001)
  - [8] D.M. Asnel et al., Phys. Rev. **D61**, 012002 (1999)
  - [9] Particle Data Group, Phys. Rev. **D66**, 012001 (2002)
  - [10] J. Boyer et al., Phys. Rev. **D42**, 1350 (1990)
  - [11] H. Marsiske et al., Phys. Rev. **D41**, 3324 (1990)
  - [12] M. Boglione and M.R. Pennington, Eur. Phys. J. **C9**, 11 (1999)
  - [13] J. Zabierowski et al., Phys. Scripta **T99**, 159 (2002)
  - [14] W. Brodowski et al., Phys. Rev. Lett. **88**, 192301 (2002)
  - [15] J. Pätzold et al., Phys. Rev. **C67**, 052202 (2003)
  - [16] A. Starostin et al., Proc. IPN Orsay Workshop Chiral Fluct. Hadr. Matter (eds. Z. Aouissat et al.), 33 (2001)
  - [17] H. Calén et al., Phys. Lett. **B366**, 39 (1996)
  - [18] M. Abdel-Bary et al., Eur. Phys. J. **A16**, 127 (2003)
  - [19] J. Bystricky et al., J. Phys. **48**, 1901 (1987) and references therein
  - [20] I. Koch, PhD thesis, Uppsala University 2004
  - [21] V.V. Shklyar et al., Nucl. Phys. **A628**, 255 (1998)
  - [22] A.I. Smirnov, Yad Fiz. **25**, 1030 (1977) (Sov. J. Nucl. Phys. **25**, 548 (1977))
  - [23] M.M. Kaskulov et al., to be published
  - [24] E. Oset et al., Prog. Theor. Phys. **103**, 351 (2000)
  - [25] M.M. Kaskulov and H. Clement, nucl-th/0401061 and Phys. Rev. C in press